Wiley
Scientifica
Volume 2024, Article ID 8212850, 20 pages
https://doi.org/10.1155/sci5/8212850

WILEY

Research Article

Characterisation of Bioactive Compounds and In Vitro Anticancer and Anthelmintic Activities of *Ilex khasiana*, an Endangered Species of Holly From Mizoram, India

Charles Lalnunfela,[1] **P. B. Lalthanpuii**,[2] **H. T. Lalremsanga**,[1] **Zothansiama**,[1] **C. Lalmuansangi**,[1] **N. Senthil Kumar**,[3] **T. C. Lalhriatpuii**,[4] **and Kholhring Lalchhandama**[2]

[1]*Department of Zoology, Mizoram University, Tanhril 796004, India*
[2]*DBT-Builder National Laboratory, Department of Life Sciences, Pachhunga University College, Aizawl 796001, India*
[3]*Department of Biotechnology, Mizoram University, Tanhril 796004, India*
[4]*Department of Pharmacy, Regional Institute of Paramedical and Nursing Sciences, Zemabawk 796017, India*

Correspondence should be addressed to Charles Lalnunfela; c.lalnunfela@gmail.com and Kholhring Lalchhandama; chhandama@pucollege.edu.in

Received 13 April 2024; Revised 4 July 2024; Accepted 27 November 2024

Academic Editor: Vishal Ahuja

Copyright © 2024 Charles Lalnunfela et al. This is an open access article distributed under the Creative Commons Attribution License, which permits unrestricted use, distribution, and reproduction in any medium, provided the original work is properly cited.

Ilex khasiana Purkay. is a critically endangered species of holly found only in Khasi Hills and Mizoram, Northeast India. Of its several medicinal uses in the Khasi and Mizo traditional systems, the anticancer and anthelmintic applications remain unexplored. A methanol extract (IKM) and three fractions, namely, butanol (IKM-B), diethyl ether (IKM-D) and hexane (IKM-H) extracts were prepared from the leaves. Cytotoxicity tests were performed in vitro on malignant human alveolar adenocarcinoma (A549) and human colorectal carcinoma (HCT116) cell lines using the 3-(4,5-dimethylthiazol-2-yl)-2,5 diphenyltetrazolium bromide (MTT) reduction reaction. All the extracts exerted inhibitory efficacy in the order, IKM-D > IKM-B > IKM > IKM-H. IKM-D was the most efficacious extract exhibiting the half-maximal inhibitory concentration (IC_{50}) values of 26.9, 64.04 and 28.61 μg/mL against A549 cells, and 22.77, 69.41 and 18.37 μg/mL against HCT116 cells at 24, 48 and 72 h, respectively. The most bioactive extract, IKM-D, was used for further anticancer tests. It induced apoptosis as indicated by red fluorescence in the dead cells. The apoptotic index values were determined at 33.5, 55.18 and 57.62 in A549 cells, and 32.47, 54.29 and 62.55 in HCT166 cells at the corresponding concentrations of 25, 50 and 100 μg/mL. It also caused significant clonogenicity by repressing cancer proliferation, but only at a concentration of 100 µg/mL. Surviving fractions of the cancer cells following extract treatment at 25, 50 and 100 μg/mL were 52.16%, 47.56% and 21.77% for A549 cells, and 52.56%, 48.12% and 8.42% for HCT116 cells. The plant extract also caused concentration-dependent inhibition of colony formation against both cell lines. Anthelmintic activity was demonstrated in an intestinal cestode, *Raillietina galli*. Scanning electron microscopy revealed hallmark anthelmintic alterations on the body parts of the parasite. The GC-MS analysis showed that the plant extract is mainly composed of a phenol, 2,6-di-tert-butylphenol. High-performance thin-layer chromatography (HPTLC) fingerprinting and quantification indicated the presence of β-sitosterol at an amount of 198.68 ng. The two compounds were predicted by computational modelling to have high binding potentiality on β-tubulin, a common anticancer and anthelmintic target. The findings established that *I. khasiana* leaves contain bioactive principles that caused inhibitory effects on carcinoma cells and produced anthelmintic effects on cestode parasite. The study advocates further investigations into the identification of the exact molecules, the precise mode of actions and therapeutic tests, as well as the need for conservation of the rare species of holly.

Keywords: anthelmintic; anticancer activity; cancer cell; cestode; Mizo traditional medicine

1. Introduction

A multifactorial disease, cancer, is one of the most perplexing medical conditions in terms of management and remediation due to a complex interplay of cell signalling systems, metabolic pathways, immune responses and diverse environmental cues involved [1]. Not a single therapy, or even a regiment of treatments, does not offer complete cure or alleviation of the associated morbidity in various forms of cancers. Novel drugs and new combinations of therapies are in relentless demand to counter the debilitating manifestations of the disease, especially to keep clinical care at par with the pervasive drug resistance in different cancer cells [2, 3]. Secondary metabolites of plants are established to be among the best sources of anticancer pharmaceutical drugs. Some of the most reliable cancer medications are known and developed from traditional medicines from substantiated medicinal plants [4, 5]. The most widely used prescription anticancer drugs are the vinca alkaloids, namely, vinblastine and vincristine, that are discovered and obtained from the periwinkle plant, *Catharanthus roseus*, traditionally known from Ayurveda. Another common drug, paclitaxel, is a tetracyclic diterpenoid derived from the bark of Pacific yew, *Taxus brevifolia*. The vinca alkaloids and paclitaxel are microtubule-targeting agents and prevent protein polymerisation by competitively binding to β-tubulin, thereby inhibiting mitotic proliferation [6]. An indole alkaloid, camptothecin, from the stem wood of *Camptotheca acuminata*, which is used in the traditional Chinese medicine, has been employed as a base molecule for the synthesis of several anticancer drugs [7]. Other plant metabolites are under investigations, including curcumin, epigallocatechin gallate and resveratrol (polyphenols) [8], kaempferol and quercetin (flavonoids), artemisinin (sesquiterpene lactone), betulinic acid (pentacyclic triterpene), gingerol (β-hydroxy ketone) and rutin (flavonol glycoside) [9]. Therefore, it is crucially vital for research attentions to focus on unexplored traditional medicines in search of novel lead molecules from botanical sources.

Of the family Aquifoliaceae, members of the genus *Ilex* representing the only surviving group, and many of them are well known in the traditional medicines of Asia and South America [10]. In traditional Chinese medicine, bitter tea prepared from *I. kudingcha* and *I. latifolia* are widely used for the treatments of diarrhoea, haematologic disorders, liver cirrhosis, myalgia and pyrexia [11]. *I. pubescens* is extensively studied as it is traditionally used in the treatment of bronchial asthma, coronary artery disease, hepatitis, high cholesterol, and hypertension [12]. Its bioactive metabolites have been reported to have anticancer [13], analgesic, anti-inflammatory [14], anticoagulant [15] and neuroprotective activities [16]. *I. paraguariensis* is a common refreshing drink commercialised as yerba mate tea in South American and is medicinally used as a therapy of cancer, inflammation and obesity [17]. Experiments have validated the anticancer property against various cell lines [18, 19].

I khasiana Purkay. is a large and rare tree endemic to Northeast India, originally described from the Khasi Hills in Meghalaya in 1938 [20]. It has been categorised in the IUCN Red List of Threatened Species as critically endangered. A localised and natural distribution had been identified in Aizawl, Mizoram, and was reported in 2019 [21]. It is an evergreen species growing up to 20 m in height. In the Khasi traditional system, a mixed extract of the bark and root is acclaimed to be potent curative for tuberculosis and viral infections. The Mizo folk healers have asserted the usefulness of the leaves against a plethora of ailments, including different microbial and parasitic infections, cancer and blood diseases. The plant's antiparasitic activity was the first of the medicinal application investigated and elucidated [22], with a subsequent demonstration of the anti-inflammatory and analgesic activities [23]. Its purported uses as a cancer therapy and as an anthelmintic have never been widely known, or systematically explored; hence, a study on its chemical property and possible effects on cancer cell lines and helminths became a stimulating vista of experimental scrutiny.

2. Materials and Methods

2.1. Chemicals. All chemicals were of standard analytical grades. Acetonitrile, agarose, ethylenediamine tetra-acetic acid, L-glutamine, methanol, phenol red, trichloroacetic acid, trizma base and trizma hydrochloride were obtained from Sigma-Aldrich Chemicals Private Limited, Bangalore, India. All other chemicals were procured from HiMedia Laboratories Private Limited, Mumbai, India. Anthelmintic drug albendazole (Zenlee) was manufactured by UNI-PEX Pharmaceutical Private Limited, New Delhi, India.

2.2. Plant Identification and Extraction. I. khasiana is known in Mizoram, India, only at Luangmual, a locality within Aizawl, located at 23°44.556′N and 92°41.956′E, from where the specimens were collected. Specimen validation was done by taxonomists at the Botanical Survey of India, Eastern Regional Office, Shillong, Meghalaya, and a voucher (bearing accession code BSI/EC/Tech./2008/577) is maintained at the Department of Pharmacy Herbarium Section, Regional Institute of Paramedical and Nursing Sciences, Mizoram, India. The leaves were collected, washed and dried in shade at room temperature (24 ± 1°C). Extraction was done using methanol (relative polarity of 0.762) in a Soxhlet apparatus of 5-L capacity continuously for 3 days. To concentrate the extract, the solvent was evaporated and recovered in a pressurised rotary vacuum evaporator (Buchi Rotavapor R-215, Flawil, Switzerland).

Three fractions were prepared from the crude methanol extract using solvents of high, medium and low polarities, namely, butanol (relative polarity of 0.586), diethyl ether (relative polarity of 0.117) and hexane (relative polarity of 0.009). In brief, 250 mL of the solvents were mixed with equal volumes of the crude extract in a separating funnel.

The solutions were added until a clear suspension of the solvents was formed. After refluxing for 4 h, the aqueous solution at the bottom and solvent fraction on top were allowed to settle down and collected in separate flasks. The fractions were concentrated in a rotary vacuum evaporator as before. After complete fractionation, four extracts were obtained, namely, the methanol (hereafter designated as IKM), butanol (IKM-B), diethyl ether (IKM-D) and hexane (IKM-H) extracts.

2.3. Cell Lines and Culture. Malignant type II human alveolar adenocarcinoma (A549) and human colorectal carcinoma (HCT116) cell lines were used to evaluate the anticancer activity of *I. khasiana* extracts. Both the cell lines were preserved at and provided by the National Centre for Cell Sciences (NCCS) at Pune, India. Minimal essential medium (MEM, composed of $CaCl_2$, KCl, $MgSO_4$, NaCl, Na_3PO_4, $NaHCO_3$ and amino acids), supplemented with 10% foetal bovine serum (FBS), 50 µg/mL gentamicin and 1% L-glutamine, was used to maintain the stock cultures using 25 cm^2 culture flasks in a humidified gas incubator (Eppendorf AG, Germany).

2.4. Cytotoxicity Assay. Anticancer efficacy was assessed using cytotoxic activity on the cancer cell lines based on 3-(4,5-dimethylthiazol-2-yl)-2,5 diphenyltetrazolium bromide (MTT) reduction reaction [24]. Approximately 10^4 A549 and HCT116 cells were seeded into 96-well culture plates containing 100 µL MEM. They were incubated in a carbon dioxide incubator maintained at 37°C ± 1°C, an atmosphere of 5% CO_2 and with 95% moisture. Initial incubation was for 24 h to allow maximum cell adherence, after which the cells were treated with varying concentrations, *viz.*, 50, 100, 200, 300 and 500 µg/mL of *I. khasiana* extracts. A control group was maintained without any treatment. The assay was ceased at 24, 48 and 72 h for each test by washing the cells with FBS-free MEM. 10 µL of MTT (5 mg/mL) was added to each sample to develop purple formazan crystals after incubating at 37°C ± 1°C for 2 h. The crystals were dissolved in 100 µL of dimethyl sulfoxide, and the solution was incubated at 37°C ± 1°C for 30 min. Each test was performed in triplicate. The absorbances of the final solutions were measured in a microplate reader (SpectraMax M2e, Molecular Devices, California, the United States of America) at the wavelength of 560 nm. The most effective extract based on the best treatment time was selected for further experiments. Cytotoxicity was determined as a percentage of inhibition from the following equation:

$$\text{Inhibition}\,(\%) = \left[\frac{\text{Control} - \text{Treatment}}{\text{Control}}\right] \times 100. \quad (1)$$

2.5. Apoptotic Assay. Cell death was studied by dual fluorescent staining method using acridine orange and ethidium bromide [25]. 1×10^5 of both A549 and HCT116 cells were plated onto six-well culture plates containing MEM. They were incubated at 37°C ± 1°C for 24 h for cell adhesion. Then, they were treated with *I. khasiana* extract for another 24 h. Control cells were maintained without the plant extracts. After completion of the treatment, the plates were washed with phosphate-buffered saline (PBS). Cells were allowed to detach by adding 0.25% trypsin–ethylenediaminetetraacetic acid (1X). 100 µL of FBS-free MEM was added to the cell pellet to obtain a cell suspension. 2.5 µL each of acridine orange (100 µg/mL) and ethidium bromide (100 µg/mL) were added to 25 µL cell suspension, and staining was allowed for 2 min. The cell suspension was spread on a glass slide and visualised using a fluorescent microscope (Invitrogen EVOS FL auto 2, Waltham, the United States of America). The apoptotic index was estimated by scoring a minimum of 300 cells based on the following equation:

$$\text{Apoptotic index}\,(\%) = \frac{[\text{Apoptotic cells scored} \times 100]}{\text{Total cells scored}}. \quad (2)$$

2.6. Clonogenic Assay. The efficacy of *I. khasiana* extracts to inhibit cell proliferation and colony formation was determined against A549 and HCT116 cells [26]. Approximately 200 cells were cultured in 5 mL MEM in Petri dishes. After incubating for 24 h at 37°C ± 1°C for cell adherence, the plant extract was added and then incubated again for 24 h. The cells were washed with PBS and resumed culturing for another 11 days in fresh media. The cells were then stained with 1% crystal violet prepared in methanol. After staining for 30 min, they were observed under an inverted microscope (Invitrogen EVOS XL Core imaging system, Waltham, the United States of America) to enumerate the colony formation. To determine the total clonogenicity, plating efficiency (PE) and surviving fraction (SF) of the cells were estimated from the following formulae:

$$\text{PE} = \frac{[\text{Number of colonies} \times 100]}{\text{Number of cells seeded}}. \quad (3)$$

$$\text{SF} = \left[\frac{\text{Number of colonies}}{\text{Number of cells seeded}}\right] \times \text{Mean PE}. \quad (4)$$

2.7. Anthelmintic Susceptibility Assay. Anthelmintic activity was evaluated against a gastrointestinal cestode, *Raillietina* (*Taenia* Mégnin, 1881) *galli* Yamaguti, 1935, based on helminth survival assay [27]. The cestodes were collected from an intestine of chicken, *Gallus gallus*. The efficacy was tested in comparison to albendazole at 20 mg/mL, a standard manufactured dosage, in a microbiological incubator at 37°C ± 1°C. Culture medium consisting of 0.9% neutral PBS supplemented with 1% dimethyl sulfoxide was taken as a negative control. The cestodes were prepared for scanning electron microscopy following the standardised method for helminths [28]. The cestodes were first fixed in 10% neutral-buffered formaldehyde, postfixed in osmium tetroxide, dehydrated in acetone, stabilised in tetramethylsilane, coated with gold and finally observed under a scanning electron microscope (JSM-6360, JEOL Ltd., Tokyo, Japan).

2.8. GC-MS Analysis. The most bioactive extract, IKM-D, was analysed for its metabolite composition in a single quadrupole TRACE 1300 ISQ LT gas chromatography-mass spectrometer (Thermo Scientific, Waltham, the United States of America). Methanol was used as the solvent. A nonpolar column TR-5MS with a dimension of 30 m length × 0.25 mm width × 0.25 μm film thickness was the stationary phase. The carrier gas, helium, was injected at 1 mL/min at a splitting ratio of 1:50. The oven temperature was raised to 250°C starting from 70°C with an increment of 10°C every 10 min. The temperatures of the ion source and transfer line were set at 250°C. The mass spectrometer was run for 32 min. Chemical data were generated using Thermo Scientific Xcalibur software and identified from the libraries of Wiley Registry and the National Institute of Standards and Technology based on chemical formulae, molecular mass and retention values.

2.9. Chromatographic Fingerprinting. Chemical fingerprinting was performed using high-performance thin-layer chromatography (HPTLC) [29]. Nine reference compounds were chosen that included asiatic acid (triterpene), boswellic acid (triterpene), chebulagic acid (tannin), chlorogenic acid (caffeic acid ester), ellagic acid (phenol), ferulic acid (phenol), gallic acid (phenol), quercetin (flavonoid) and β-sitosterol (steroid). A working concentration of 50 µg/mL was prepared for each compound. The compounds and IKM-D were loaded in 10 mm bands on precoated TLC plates on the aluminium sheet embedded with silica gel 60 coupled with the fluorescence indicator F_{254} (Merck KGaA, Darmstadt, Germany), having layer thickness of 250 μm and size 20 × 10 cm. Sample application was done with CAMAG Linomat 5 applicator coupled to CAMAG HPTLC system (Muttenz, Switzerland). The plates were developed in CAMAG twin-trough chamber using the appropriate mobile phases (Table 1). The plates were removed when the solvent front reached 7 cm, air-dried and scanned in CAMAG TLC Scanner 4 winCATS software (Cordial Versicherungs–Dienstleistungen GmbH, Hannover, Germany). For compound quantification, 2, 4, 6, 8, 10, 12 and 14 µL of standard compounds were applied on TLC plates at the speed of 150 nL/sec. 4 µL of *I. khasiana* extract (prepared at 50 mg/mL) was similarly put on a TLC plate. The developing chamber was presaturated with a mobile-phase solvent mixture of toluene:methanol (16:2 v/v) for 15 min. Chromatographic migration was allowed on the TLC plates when the mobile phase attained a distance of 7 cm. Scanning was done at 254 nm wavelength, in a slit width of 5 × 0.45 mm, with a scanning speed of 40 mm/s and data resolution at 50 µm/step using a deuterium lamp.

2.10. Molecular Docking. To predict the molecular interaction of 2,6-di-tert-butylphenol and β-sitosterol, the three-dimensional (3D) structures were retrieved from PubChem (https://pubchem.ncbi.nlm.nih.gov), the US National Centre for Biotechnology Information (NCBI), and saved in structured data file (SDF) formats. Structure optimisation and cumulative potential energy minimisation were performed on ChemBio3D Ultra 12.0 (CambridgeSoft Corporation, Cambridge, the United States of America) using the force field MMFF94. The compounds were docked to the protein β-tubulin, a common molecular target of major anthelmintic and anticancer drugs. The X-ray diffraction structure of β-tubulin was obtained from the Research Collaboratory for Structural Bioinformatics (RCSB) protein data bank (RCSB-PDB) (https://www.rcsb.org, PDB code 1SA0) [30]. To avoid unwanted chemical interruptions, molecules associated with the protein such as cofactors, water and unique ligands were removed using Molegro Molecular Viewer software. Molecular docking was done on the AutoDock Vina v1.2.4 platform (Molecular Graphics Lab, The Scripps Research, La Jolla, the United States of America) [31]. Polar hydrogens and Kollman charges were added using the Molecular Graphics Lab biosoftware MGLTools 1.5.6 before saving the data in protein data bank, partial charge (Q) and atom type (T) (PDBQT) format.

Table 1: Inhibitory activity of *I. khasiana* extracts prepared from different solvents against A549 cells recorded at daily intervals.

Extract	Solvent polarity	IC_{50}		
		24 h	48 h	72 h
IKM	5.1	202.50 ± 4.53	195.77 ± 4.15	162.27 ± 5.30
IKM-B	3.9	134.90 ± 7.64	077.98 ± 6.55	052.74 ± 5.66
IKM-D	2.8	026.90 ± 6.08	064.04 ± 3.27	028.61 ± 7.44
IKM-H	0.1	257.70 ± 6.98	216.13 ± 7.32	192.50 ± 9.67

Note: Values in means ± standard error of the means; IKM: *I. khasiana* methanol extract; IKM-D: diethyl ether fraction of IKM; IKM-B: IKM butanol fraction of IKM; IKM-H: hexane fraction of IKM.

2.11. Statistical Analysis. All data were expressed as means ± standard error of means. Statistical differences were determined by one-way analysis of variance (ANOVA) followed by Tukey's post hoc test using GraphPad Prism 8.0 (Insight Partners, New York, the United States of America). The half-maximal inhibitory concentration (IC_{50}) was determined from the log doses generated from GraphPad Prism. Clonogenicity and anthelmintic efficacy were compared between the test group against the controls by Student's t-test with a significant difference taken at $p < 0.05$.

3. Results

3.1. Cytotoxicity. Cytotoxic efficacy of *I. khasiana* extracts was assessed on A549 and HCT116 cells. A549 cells were responsive to all the plant extracts as shown in Figure 1. The cells responded well to all the extracts, with the order of inhibitory efficacy as IKM-D > IKM-B > IKM > IKM-H (Table 1 and Figure 2). IKM-D was by far the most effective extract, indicating IC_{50} values of 26.9, 64.04 and 28.61 µg/mL at 24, 48 and 72 h, respectively. IKM-H showed the least activity with IC_{50} values of 257.7, 216.13 and 192.5 µg/mL at the three-hour intervals, respectively.

The cytotoxic responsiveness of HCT116 cells to *I. khasiana* extracts is depicted in Figure 3, and the comparative inhibitory efficacy is presented in Table 2 and

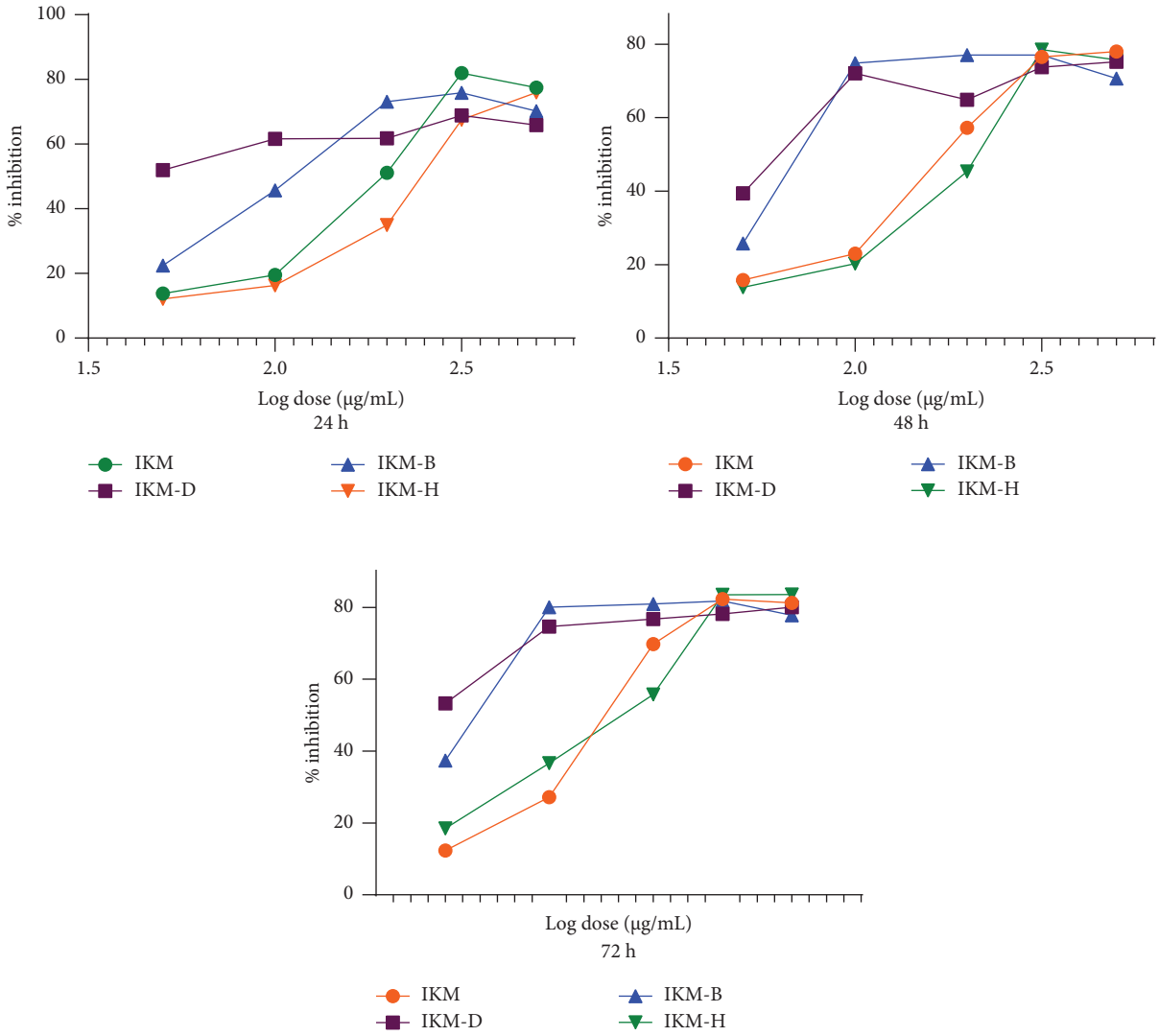

Figure 1: Inhibitory effect of *I. khasiana* extracts against human alveolar adenocarcinoma (A549) cell line after treatment for 24, 48 and 72 h. IKM: *I. khasiana* methanol extract; IKM-D: diethyl ether fraction of IKM; IKM-B: IKM butanol fraction of IKM; IKM-H: hexane fraction of IKM.

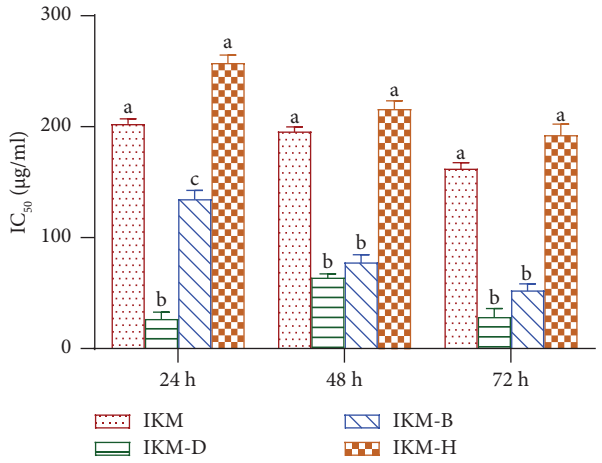

Figure 2: IC_{50} of *I. khasiana* extracts on A549 cells after treatment for 24, 48 and 72 h. IKM: *I. khasiana* methanol extract; IKM-D: diethyl ether fraction of IKM; IKM-B: IKM butanol fraction of IKM; IKM-H: hexane fraction of IKM. Values are expressed as means ± standard error of the means. Same letters on the bars indicate significant variation (<0.05) between the test groups; different letters are not significant.

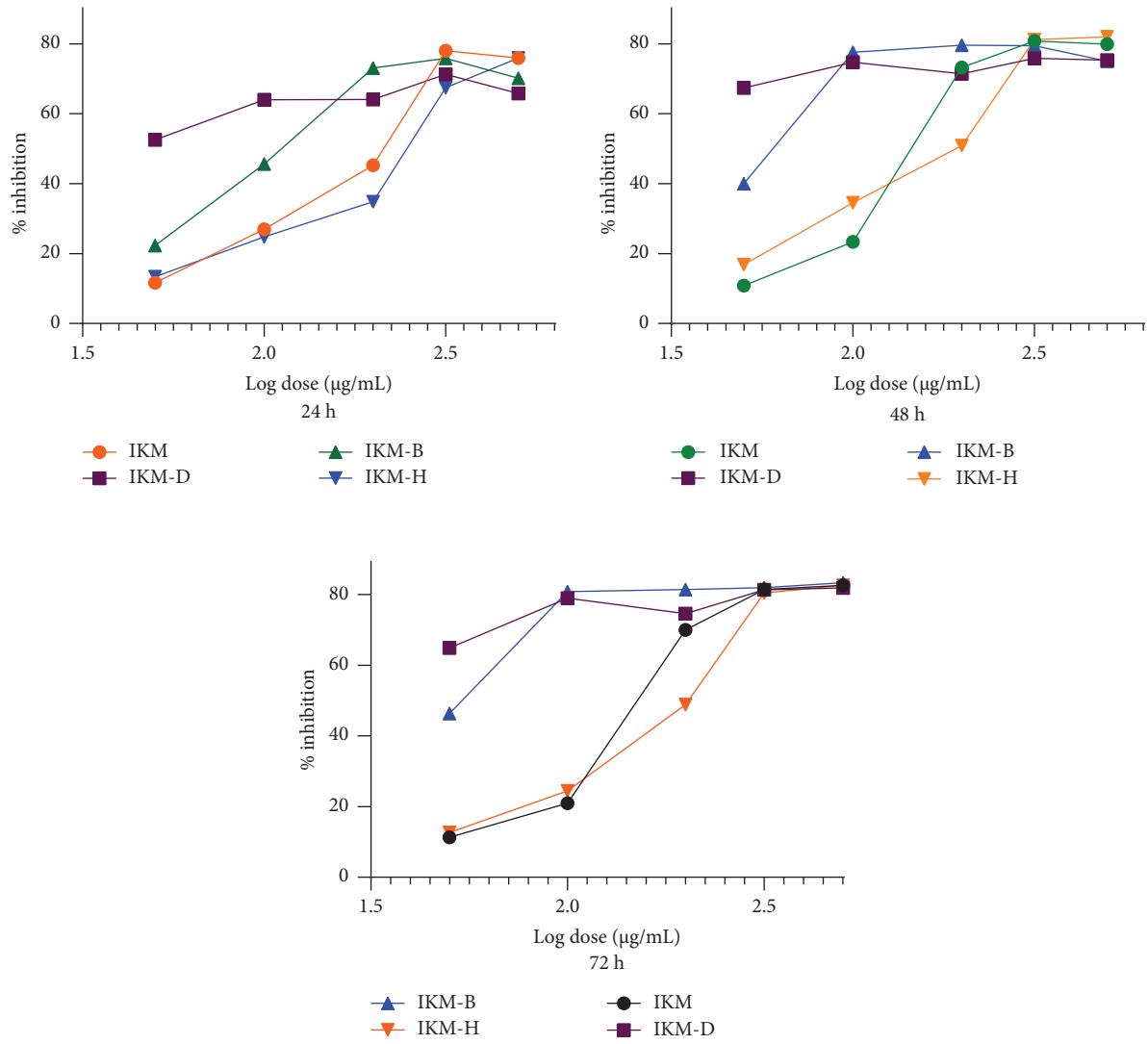

Figure 3: Inhibitory effect of *I. khasiana* extracts against colorectal carcinoma cell line (HCT116 cells) after treatment for 24, 48 and 72 h. IKM: *I. khasiana* methanol extract; IKM-D: diethyl ether fraction of IKM; IKM-B: IKM butanol fraction of IKM; IKM-H: hexane fraction of IKM.

Table 2: Inhibitory activity of *I. khasiana* extracts prepared from different solvents against HCT116 cells recorded at daily intervals.

Extract	Solvent polarity	IC_{50}		
		24 h	48 h	72 h
IKM	5.1	222.73 ± 7.14	153.90 ± 6.50	157.87 ± 8.90
IKM-B	3.9	135.10 ± 8.34	048.28 ± 6.25	040.51 ± 9.21
IKM-D	2.8	022.77 ± 4.68	069.41 ± 3.49	018.37 ± 3.53
IKM-H	0.1	255.90 ± 7.45	206.53 ± 4.76	265.87 ± 4.75

Note: Values in means ± standard error of the means; IKM: *I. khasiana* methanol extract; IKM-D: diethyl ether fraction of IKM; IKM-B: IKM butanol fraction of IKM; IKM-H: hexane fraction of IKM.

Figure 4. IKM-D was again the most cytotoxic showing IC_{50} of 22.77, 69.41 and 18.37 μg/mL at 24, 48 and 72 h, respectively. However, at 48 h treatment, IKM-B (at 48.28 μg/mL) and IKM-C (at 68.9 μg/mL) showed better inhibition as indicated by higher IC_{50} values. The overall result indicates that IKM-D has the most potent cytotoxicity among the different extracts used and therefore was most suitable for all the subsequent biological and chemical assays.

3.2. Cell Death. Cancer cells were exposed to 25, 50 and 100 μg/mL of IKM-D, and any change in cell appearance was examined and compared with that of untreated (control) cells under a fluorescent microscope. The fluorescent micrographs of A549 and HCT116 cells are shown in Figures 5 and 6, respectively. Live cells were distinctively captured with bright-green fluorescence due to acridine orange uptake indicating intact cytoplasmic and nuclear organisations

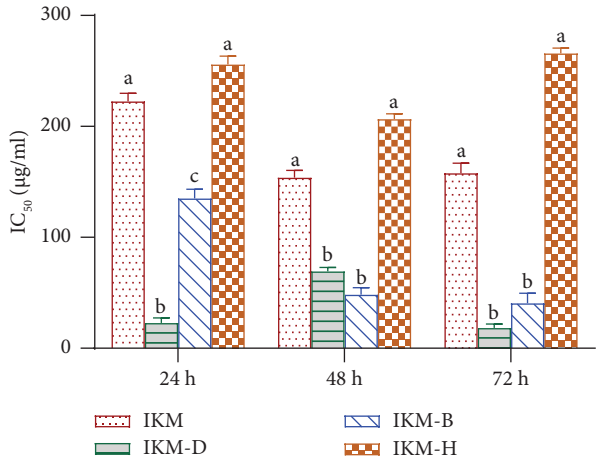

FIGURE 4: IC_{50} of selected *I. khasiana* extracts on HCT116 cells after treatment for 24, 48 and 72 h. IKM: *I. khasiana* methanol extract; IKM-D: diethyl ether fraction of IKM; IKM-B: IKM butanol fraction of IKM; IKM-H: hexane fraction of IKM. Values are expressed as means ± standard error of the means. Same letters on the bars indicate significant variation ($p < 0.05$) between the test groups; different letters are not significant.

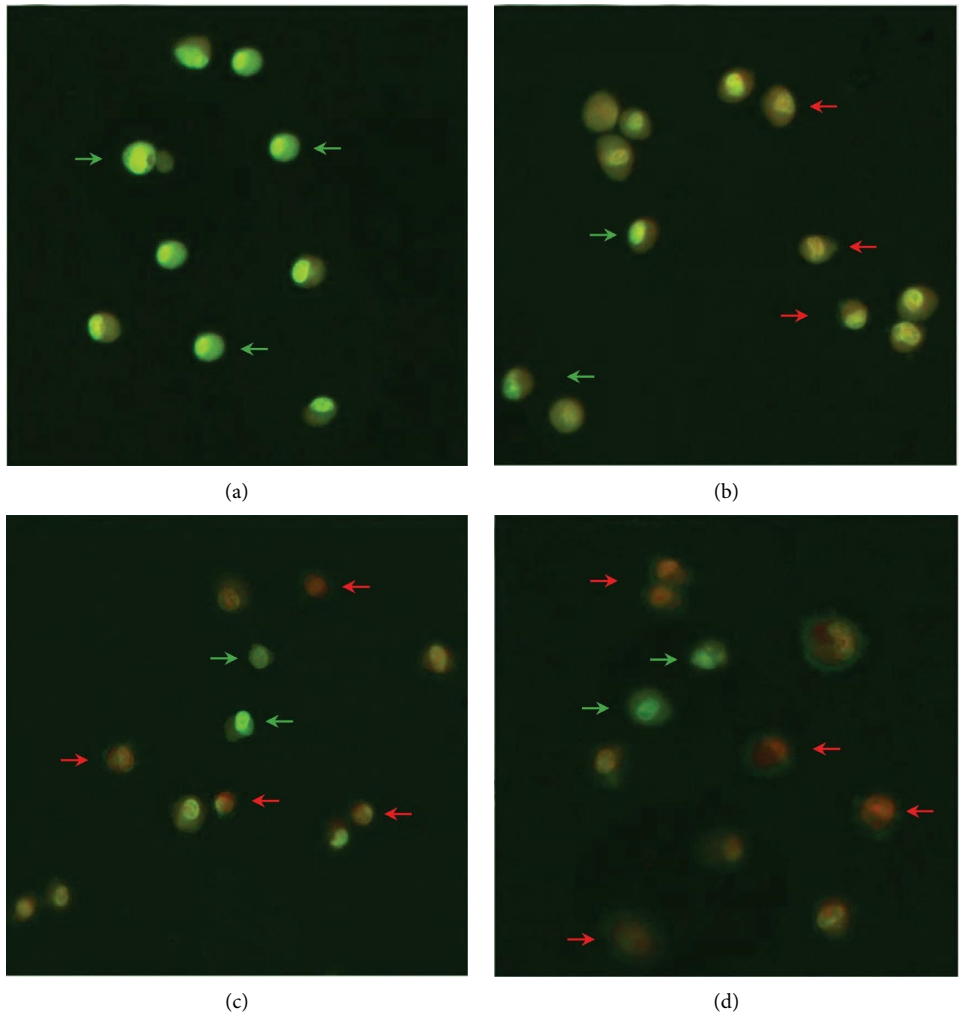

FIGURE 5: Fluorescent micrographs of A549 cells dual stained with acridine orange and ethidium bromide after treatment with IKM-D for 24 h. Green arrows point to live cells that displayed green fluorescence, while red arrows indicate apoptotic cells that display reddish colouration. (a) Control, without any treatment; (b) treatment with IKM-D at 25 μg/mL; (c) treatment with IKM-D at 50 μg/mL; (d) treatment with IKM-D at 100 μg/mL.

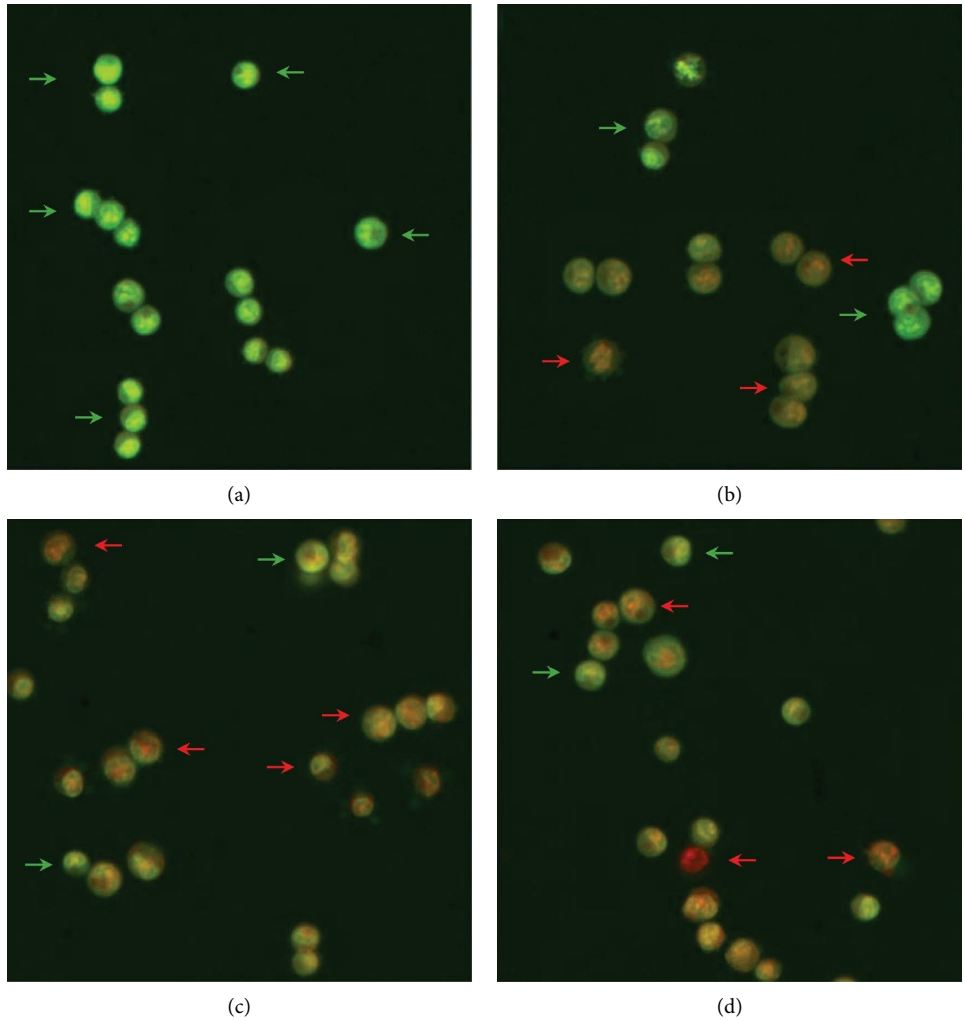

Figure 6: Fluorescent micrographs of HCT116 cells dual stained with acridine orange and ethidium bromide after treatment with IKM-D for 24 h. Green arrows point to live cells that displayed green fluorescence, while red arrows indicate apoptotic cells that display reddish colouration. (a) Control, without any treatment; (b) treatment with IKM-D at 25 µg/mL; (c) treatment with IKM-D at 50 µg/mL; (d) treatment with IKM-D at 100 µg/mL.

Table 3: Apoptotic index of *I. khasiana* methanol–diethyl ether extract (IKM-D) against carcinoma cells.

Concentration (μg/mL)	Cell line	
	A549	HCT116
25	33.50 ± 2.80	32.47 ± 1.83
50	55.18 ± 3.03	54.29 ± 2.43
100	57.62 ± 2.22	62.55 ± 2.16

Note: Values in means ± standard error of the means.

(Figures 5(a) and 6(a)). Apoptotic cell deaths were observed as showing dull red or greenish red with vivid orange–red nuclear regions, indicating nuclear chromatin fragmentation and membrane disruption as stained by ethidium bromide. The degree of colour transition in different cells reflects the stages of apoptosis, with the most reddish ones (Figures 5(d) and 6(d)) induced by the plant extract at 100 μg/mL, the most apoptotic.

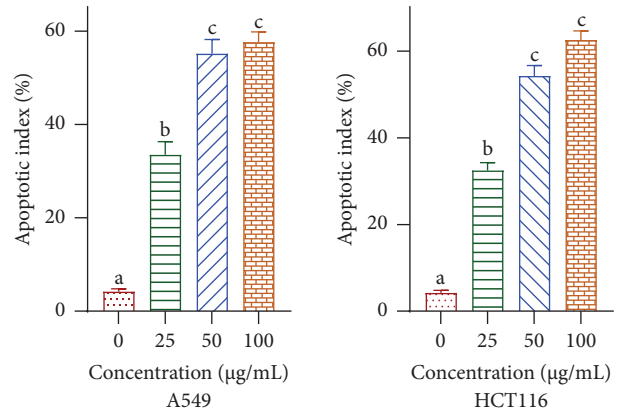

Figure 7: Apoptotic deaths of A549 and HCT116 cells after treatment with IKM-D for 24 h. Values are expressed as means ± standard error of the means. Same letters on the bars indicate significant variation ($p < 0.05$) between the test groups; different letters are not significant.

Table 4: Surviving fraction of A549 and HCT116 after treatment with *I. khasiana* methanol–diethyl ether extract (IKM-D).

Concentration (μg/mL)	Cell line	
	A549	HCT116
0	89.93 ± 1.37	87.39 ± 1.33
25	52.56 ± 3.15*	52.58 ± 2.38*
50	47.14 ± 4.30*	48.12 ± 3.30*
100	21.77 ± 0.78*	08.42 ± 0.12*

Note: Values in means ± standard error of the means.
*Significantly different at $p < 0.05$ against control.

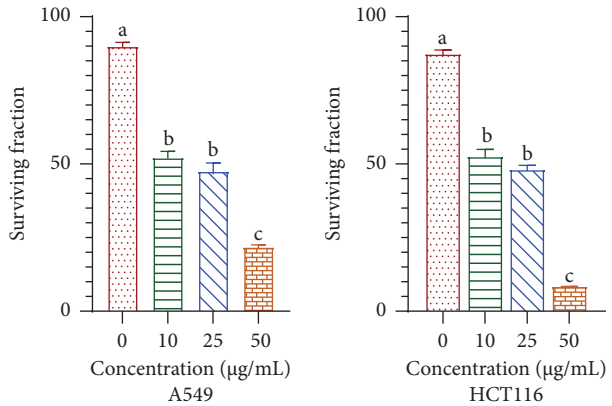

Figure 8: Inhibitory effects of IKM-D on the proliferation of A549 and HCT116 cells after treatment for 24 h. Values are expressed as means ± standard error of the means. Same letters on the bars indicate significant variation ($p < 0.05$) between the test groups; different letters are not significant.

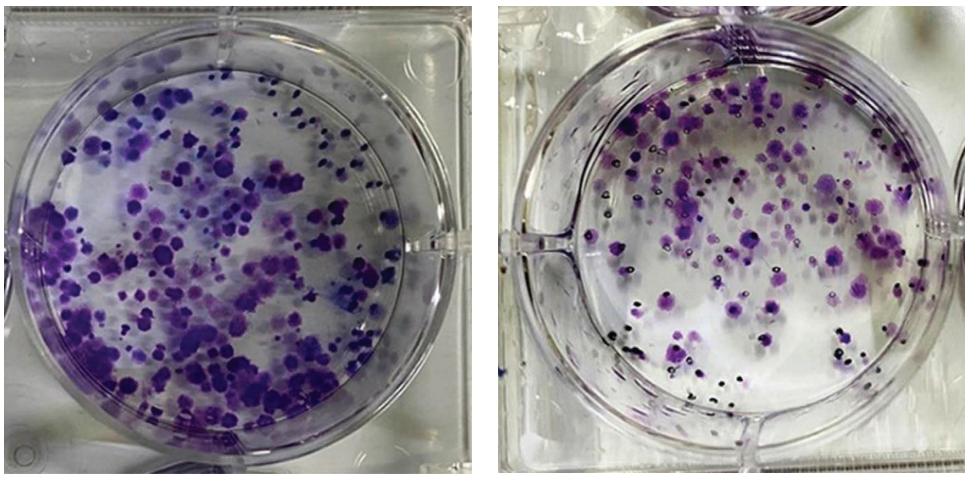

(a) (b)

Figure 9: Continued.

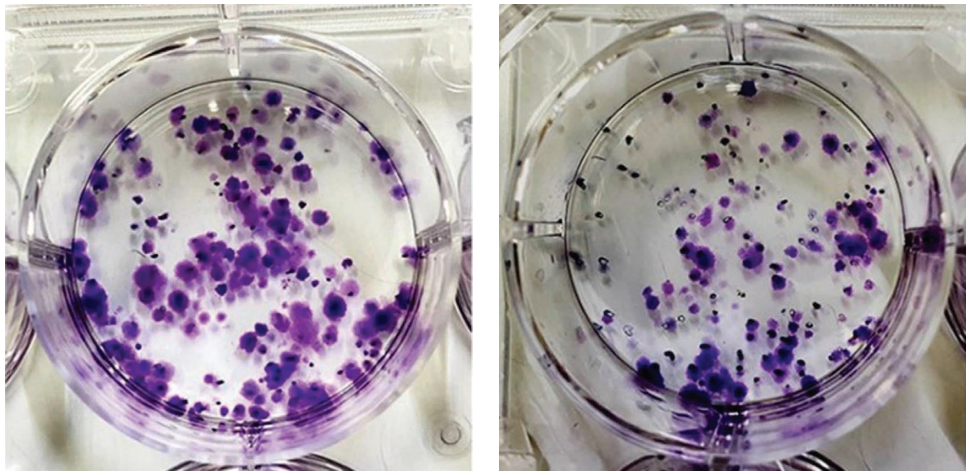

(c) (d)

Figure 9: Colony formation of A549 cells in minimal essential medium. (a) Control, without any treatment; (b) treatment with IKM-D at 25 μg/mL; (c) treatment with IKM-D at 50 μg/mL; (d) treatment with IKM-D at 100 μg/mL.

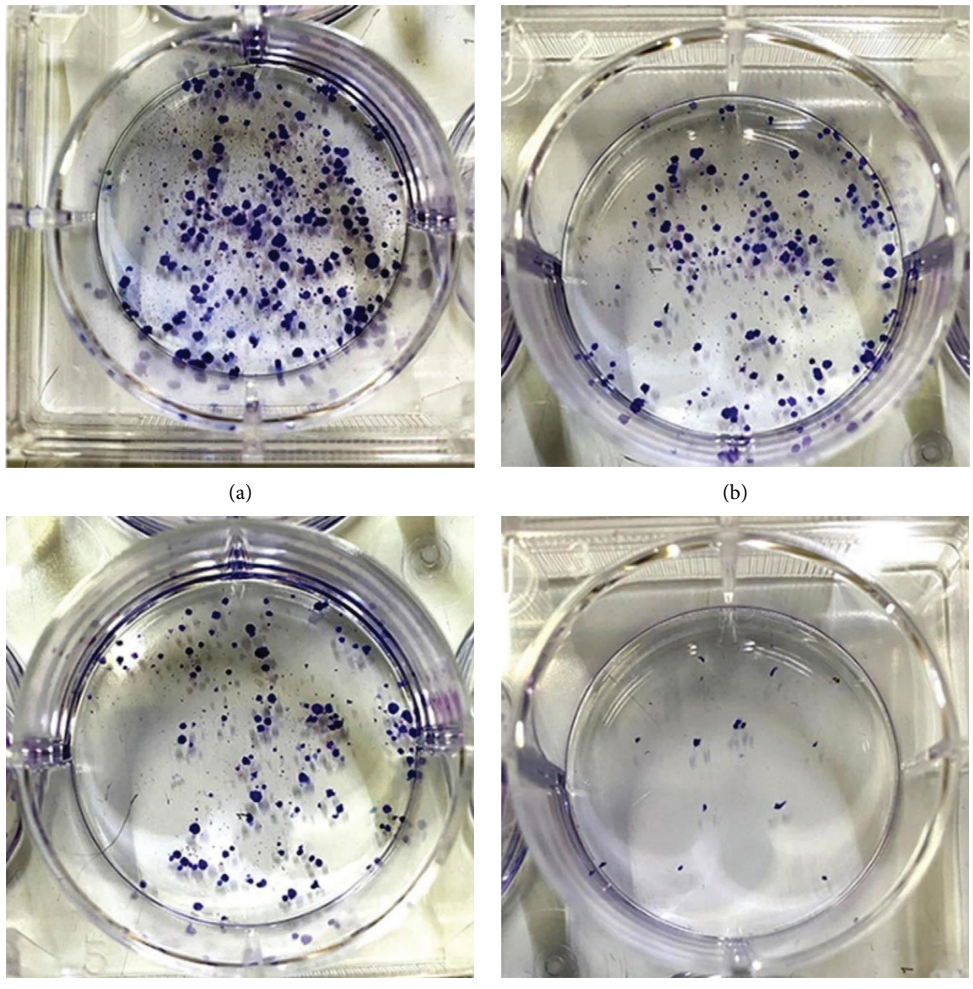

(a) (b)

(c) (d)

Figure 10: Colony formation of HCT116 cells in minimal essential medium. (a) Control, without any treatment; (b) treatment with IKM-D at 25 μg/mL; (c) treatment with IKM-D at 50 μg/mL; (d) treatment with IKM-D at 100 μg/mL.

Table 5: Anthelmintic efficacy of *I. khasiana* methanol–diethyl ether extract (IKM-D) against the cestode, *R. galli*, compared to untreated control and positive control, i.e., albendazole-treated groups.

Treatment media	Concentration (mg/mL)	Normalised survival time (h)	*t* value	*t* critical value
Negative control	0	100.00 ± 2.56	—	—
Albendazole	20	004.48 ± 0.98*	49.77	2.23
IKM-D	20	022.21 ± 2.85*	85.48	2.25

Note: $n = 6$.
*Significantly different at $p < 0.05$ against negative control.

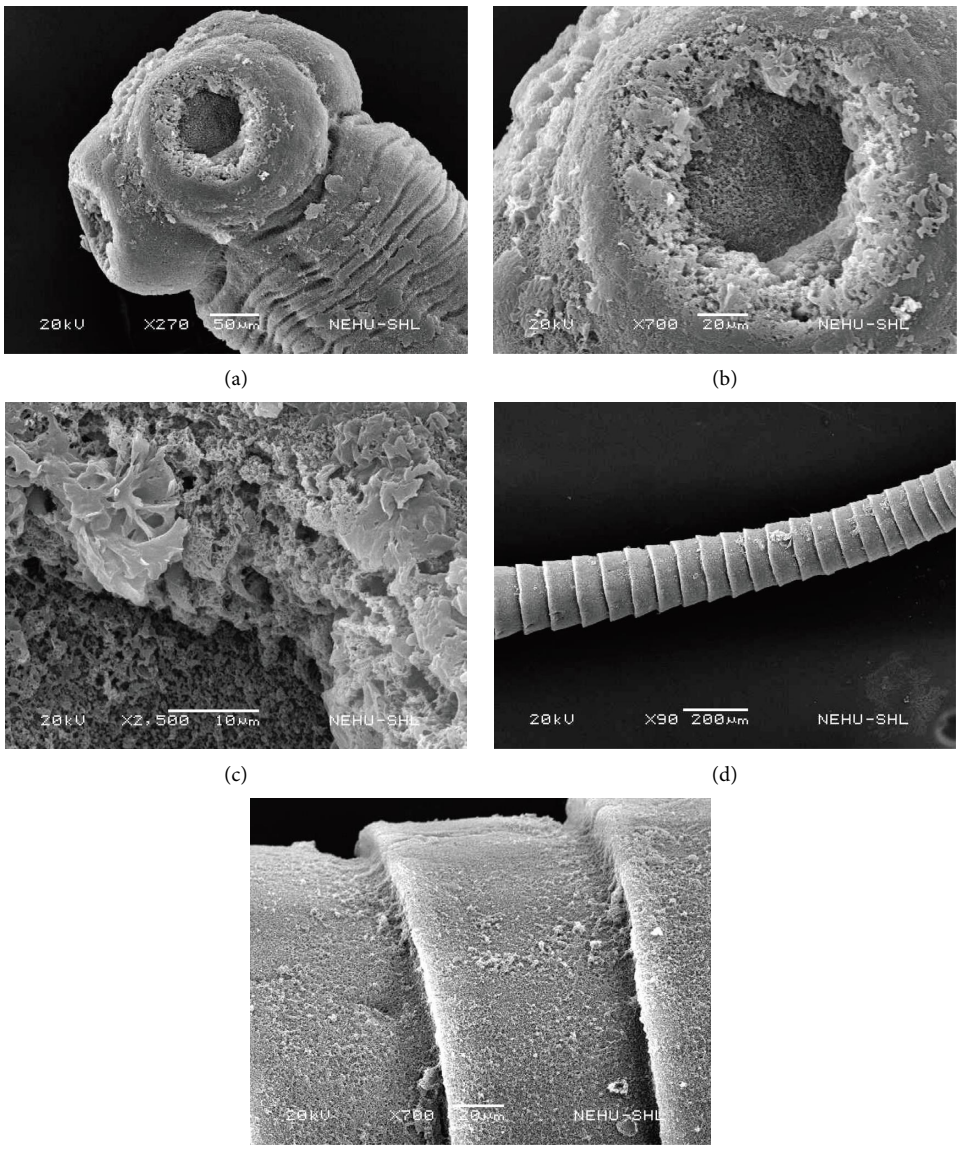

Figure 11: Scanning electron micrograph of a cestode, *R. galli*, treated with *I. khasiana* methanol–diethyl ether extract (IKM-D). (a) Anterior end of the body show a spheroidal scolex connected to the neck; ovoid suckers are located laterally. (b) A single sucker indicates extensive damage, with scraps of tissues distributed haphazardly. (c) The rim of a sucker where attachment devices called spines should normally present but instead represented by diffused tissues with two spines remaining in the middle in degraded pointy structures. (d) The main body shows a chain of body segments, proglottids. (e) Magnification of the proglottids reveals extensive disruption of the teguments which otherwise should be covered with smooth microtriches.

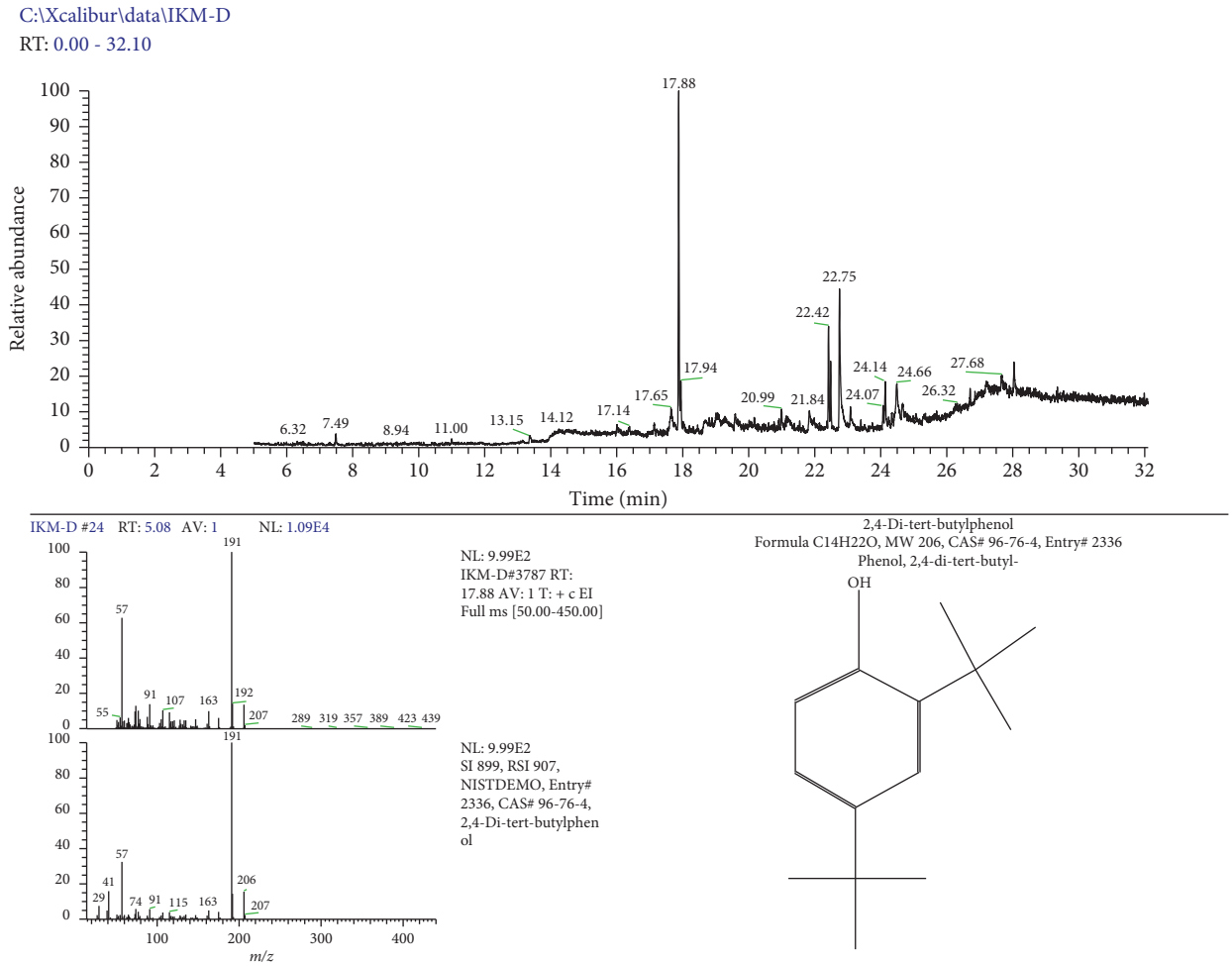

Figure 12: GC-MS chromatogram and mass spectra of *I. khasiana* methanol–diethyl ether extract (IKM-D).

The apoptotic effectiveness of the plant extract against both A549 and HCT116 cells is shown in Table 3 and Figure 7. The values of apoptotic deaths were determined as 33.5%, 55.18% and 57.62% for A549 cells, and 32.47%, 54.29% and 62.55% for HCT166 cells after treatments with 25, 50 and 100 μg/mL of the plant extract, respectively. The apoptotic index revealed dose-dependent activity of IKM-D against both the cell lines (Figure 7).

3.3. Cell Proliferation. Cell proliferation or clonogenicity of A549 and HCT116 cells under control and IKM-D treatments at 25, 50 and 100 μg/mL is shown in Table 4. The survival duration of A549 cells was 89.93 h and HCT116 cells was 87.39 h in control media consisting of MEM. Treatment with IKM-D for 11 days showed concentration-dependent growth inhibition (Figure 8). Only the extract at a concentration of 100 μg/mL indicated significant efficacy ($p < 0.5$) compared to that of the control. The surviving fractions were estimated at 52.16%, 47.56% and 21.77% for A549 cells, and 52.56%, 48.12% and 8.42% for HCT116 cells against the three concentrations of IKM-D, respectively. Concentration-dependent activity on inhibition of cell colony formation was observed as shown in Figures 9 and 10.

3.4. Anthelmintic Activity. The survival of *R. galli* in control medium and treatment with IKM-D is shown in Table 5. The plant extract was noted to cause significant anthelmintic activity in comparison with albendazole at a standard dosage, i.e., 20 mg/mL. Normalised survival times against those of the cestode in negative control indicated 1.89 ± 0.52 h in albendazole and 31.73 ± 1.21 h in IKM-D treatments. Scanning electron micrographs show that the cestode has a bulbous anterior end, called the scolex, that bears apical mouth-like rostellum and rounded suckers on the sides (Figure 11(a)). A sucker is extensively damaged with its spines, which are the main parasitic attachment organs, dislocated and the surrounding body surface (tegument) eroded (Figure 11(b)). On higher magnification, tissue necrosis appeared more pronounced on the sucker that shows disintegration of spines, with very few remaining, and massive tissue clumping of the tegument (Figure 11(c)). The main body of the cestode is

Table 6: Compounds identified from *I. khasiana* methanol–diethyl ether extract (IKM-D) using GC-MS.

Sl. no	Retention time (min)	Probability (%)	Compound	Chemical formula	Molecular weight
1	6.32	14.56	Glyceryl tridocosahexaenoate	$C_{69}H_{98}O_6$	1022
2	7.49	25.66	Dimethyl(chloromethyl)silyloxymethylbenzene	$C_{10}H_{15}ClOSi$	214
3	8.94	14.09	8,11-Octadecadiynoic acid, methyl ester	$C_{19}H_{30}O_2$	294
4	11.0	18.50	1,4-Benzenediol, 2,6-bis(1,1-dimethylethyl)	$C_{14}H_{22}O_2$	222
5	13.15	15.63	5,7-Dodecadiyn-1,12-diol	$C_{12}H_{18}O_2$	194
6	14.12	20.63	Resorcinol	$C_6H_6O_2$	110
7	17.14	26.26	5,6,7,8,9,10-hexahydro-9-phenyl-spiro[2H-1,3-benzoxazine-4,1′-cyclohexane]-2-thione	$C_{19}H_{25}NOS$	315
8	17.65	16.03	1,1-Bis(dodecyloxy)hexadecane	$C_{40}H_{82}O_2$	595
9	17.88	70.14	2,6-Di-tert-butylphenol	$C_{14}H_{22}O$	206
10	17.94	54.82	Butylated hydroxytoluene	$C_{15}H_{24}O$	220
11	20.99	14.34	[1,1′-Bicyclopropyl]-2-octanoic acid, 2′-hexyl-, methyl ester	$C_{21}H_{38}O_2$	322
12	21.84	18.88	Caffeine	$C_8H_{10}N_4O_2$	194
13	22.42	30.46	Hexadecanoic acid, methyl ester	$C_{17}H_{34}O_2$	270
14	22.75	60.89	Palmitic acid	$C_{17}H_{32}O_2$	256
15	24.07	10.30	1,2-15,16-Diepoxyhexadecane	$C_{16}H_{30}O_2$	254
16	24.14	12.45	9,12,15-Octadecatrienoic acid, 2,3-dihydroxypropyl ester	$C_{21}H_{36}O_4$	352
17	24.66	15.05	12-Methyl-E,E-2,13-octadecadien-1-ol	$C_{19}H_{36}O$	280
18	26.32	13.63	2-Bromotetradecanoic acid	$C_{14}H_{27}BrO_2$	306
19	27.68	14.59	(2-Phenyl-1,3-dioxolan-4-yl)methyl (9E)-9-octadecenoate	$C_{28}H_{44}O_4$	444

Table 7: HPTLC fingerprinting of *I. khasiana* extract (IKM-D) for bioactive compounds.

No.	Compound	TLC mobile phase	Solvent ratio	Detection
1	Asiatic acid	Toluene:ethyl acetate:formic acid	5:5:1	–
2	Boswellic acid	Acetic acid:hexane:ethyl acetate:toluene	0.3:1:8:2	–
3	Chebulagic acid	Ethyl acetate:toluene:formic acid:methanol	6:1:1:2	–
4	Chlorogenic acid	Ethyl acetate:dichloromethane:formic acid:acetic acid:water	10:2.5:1:1:1.1	–
5	Ellagic acid	Toluene:ethyl acetate:methanol:formic acid	5:4.5:3:2.5	–
6	Ferulic acid	Toluene:ethyl acetate:formic acid	5:5:0.2	–
7	Gallic acid	Toluene:ethyl acetate:methanol:formic acid	5:4.5:3:2.5	–
8	Quercetin	Toluene:ethyl acetate:formic acid	5:4:0.2	–
9	β-Sitosterol	Toluene:methanol	16:2	+

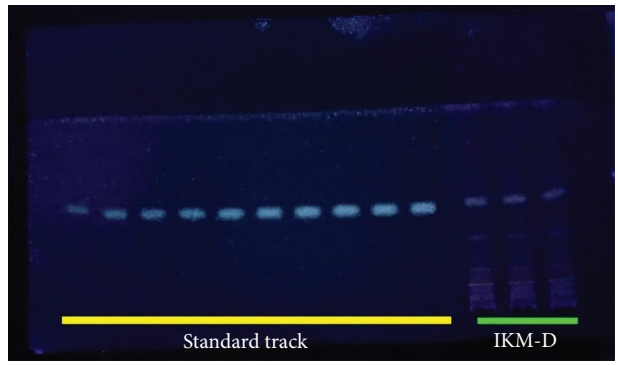

Figure 13: TLC fingerprinting shows the migration of *I. khasiana* methanol–diethyl ether extract (IKM-D) in comparison with ten-level concentrations of β-sitosterol.

Table 8: HPTLC validation parameters for β-sitosterol quantification.

Parameter	Result
Linearity (ng/band)	100–550
R_f value	0.43 ± 1
Correlation coefficient	0.99
Slope	3.05
Intercept	209.87
Limit of detection (ng/band)	42.99
Limit of quantification (ng/band)	143.28

composed of chains of segments, proglottids (Figure 11(d)). Fuzzy hair-like filaments are visible indicating disintegration of the tegumental surface (Figure 11(e)).

3.5. Chemical Profiling. The chromatogram and mass spectra of IKM-D from GC-MS are shown in Figure 12. From the mass spectral library, 19 different compounds were identified as listed in Table 6. An alkylated phenol, 2,6-di-tert-butylphenol (formula: $C_{14}H_{22}O$; molecular mass: 206.32), was determined to be the most abundant constituent, comprising 100% of the total compounds by relative abundance, and probability value of 70%. Only another compounds was in high occurrence, which was palmitic acid (formula: $C_{17}H_{32}O_2$; molecular mass: 256.42) at 60% probability and 43% relative abundance. The rest of the compounds in trace amounts were all lipids and lipid derivatives.

3.6. HPTLC Fingerprinting and Compound Quantification. From HPTLC fingerprinting, only β-sitosterol was detected in IKM-D out of the nine reference compounds (Table 7 and Figure 13). The precision and fidelity of the method applied were indicated by consistently high mean recovery percentage (> 97) for all test samples. The linear calibration curve was obtained at the range of 100–550 ng for quercetin from which a correlation coefficient was determined at 0.99 between the plant extract and β-sitosterol (Table 8). The high correlation coefficient, supported by high recovery values (all above 97.5%), further strengthened the fidelity of the procedure (Table 9). The limit of detection (LOD) reflecting the least level of the compound detectable was determined at 42.99 ng/10 mm band, while the limit of quantification (LOQ) for the lowest quantifiable amount was 143.28 ng/10 mm band. IKM-D showed an R_f value of 0.43, corresponding to that of the standard compound (Figure 14), and the total amount of β-sitosterol quantified in the extract was 198.68 ng (Table 10).

3.7. Computational Molecular Binding. Two main compounds, 2,6-di-tert-butylphenol and β-sitosterol, detected from IKM-D using GC-MS and HPTLC fingerprinting, respectively, were docked against β-tubulin, a common target protein of anticancer and anthelmintic drugs. Molecular interactions for the two compounds are prepared as shown in Table 11 and the binding sites in Figure 15. Both compounds showed quintessential binding scores against the target protein with strong deviation on negative values, a binding energy of −5.7 kcal/mol for 2,6-di-tert-butylphenol and −6.7 kcal/

Table 9: HPTLC recovery values of β-sitosterol from *I. khasiana* extract (IKM-D).

Amount (μL)	Amount (ng/band)	Expected area	Area obtained	Mean recovery (%)	Relative standard deviation (%)
4	200	2509.91	2467.11	98.29	0.29
4	300	2877.31	2806.60	97.54	0.27
4	400	3398.21	3218.12	98.70	0.32

Table 10: HPTLC quantification of *I. khasiana* extract (IKM-D).

R_f value	Mean area	Amount (μg)	Regression	Compound
0.43 ± 1	1326.10	198.68	Linear	β-Sitosterol

mol for β-sitosterol (Table 12). 2,6-Di-tert-butylphenol displayed the limited interaction site only at glycine at amino acid position 146 (Figure 15(a)). In contrast, β-sitosterol exhibited multiple binding sites, alanine and valine at two positions each and phenylalanine and tryptophan at one position each (Figure 15(b)). Thus, β-sitosterol has a more versatile interaction with β-tubulin than 2,6-di-tert-butylphenol.

4. Discussion

A549 and HTC116 cell lines are established models for the first-line experimental assessment of anticancer agents, as their molecular responses, cell cycle interruptions and biochemical processes are fairly understood [32, 33]. Knowing that these cells are highly susceptible to anticancer agents and that substantial drugs have been derived from medicinal plants after testing upon the cells, it is interesting that *I. khasiana* leaves are shown for the first time to exhibit anticancer activity. With 669 species identified, many *Ilex* are known in various traditional systems as versatile medicinal plants, with at least 38 of them claimed as a cancer therapy [34]. Different species such as *I. argentina*, *I. brasiliensis*, *I. brevicuspis*, *I. dumosa*, *I. integerrima*, *I. microdonta, I. paraguariensis*, *I. pseudobuxus*, *I. taubertiana* and *I. theezans* are commercially used as alternatives to tea in South America [11] and are specifically claimed to be preventive against cancer development [10].

I. paraguariensis is the best understood species and most used beverage. The chemical analysis showed that it is a rich source of bioactive metabolites such as caffeine derivatives (caffeic acid, chlorogenic acid, 3,4-dicaffeoylquinic acid, 3,5-dicaffeoylquinic acid and 4,5-dicaffeoylquinic acid) and flavonoids (kaempferol, quercetin and rutin) [35]. These phytocompounds are already established for their antioxidant, thereby, cancer preventive, and direct cytotoxic activity against cancer cell lines [9, 36]. *I. paraguariensis* extract has shown to have a cytotoxic effect against human colon adenocarcinoma cells (HT-29 and CaCo-2 cells) [37], urinary bladder carcinoma cell (T24), Caucasian oesophageal carcinoma cell (OE-33) (Caucasian oesophageal carcinoma) and A549 cells [38].

I. vomitoria extract reportedly exhibits cytotoxic activity against human colon adenocarcinoma cells (HT-29), while capable of acting synergistically with anticancer compounds such as caffeoylquinic acids, quercetin and kaempferol to increase cellular antioxidation reactions [39]. A popular Chinese bitter tea, *I. kudingcha*, was demonstrated as an anticancer agent and specifically regulates oncogenes such as *Bax* and *Bcl-2*, while suppressing *iNOS* and *COX-2* expressions, which are pivotal steps in carcinogenesis, in human breast adenocarcinoma (MCF-7) [40] and tongue carcinoma cells (TCA8113) [41]. *I. hainanensis* effectively inhibits several oncogenes in experimental melanoma-bearing mice [42]. Another herbal tea, *I. latifolia*, contains several phenolic and caffeic derivatives that has shown to have cytotoxicity against human cervix carcinoma HeLa cells [43]. Four novel triterpenoid saponins isolated from *I. rotunda* were found to have anticancer activity against A549, HeLa and glioblastoma (LN229) cell lines [44]. In the present study, *I. khasiana* extracts showed an unusual effect on the cancer cells that at some points there were nonlinear responses such as IKM-D on A549, and IKM, IKM-D and IKM-H on HCT116 cells. This kind of anomalous cellular response is due to dose-effect limitations and stress conditions of target cells that is a common phenomenon often seen in the effects of anticancer drugs [45] and phytocompounds [46, 47].

Identifications of two compounds form of *I. khasiana* extract, namely, 2,6-di-tert-butylphenol, as the major component from GC-MS and β-sitosterol from HPTLC fingerprinting have important implication in the plant's medicinal values. The chemistry and biological property of the compounds have attracted pharmacological investigations with valuable outcomes. 2,6-Di-tert-butylphenol is a phenolic compound and secondary metabolite of several species of bacteria and plants [48]. It is not particularly stable as a pure compound, and thus, not suitable for clinical use. It has a high antioxidant power for which it is widely used in drug synthesis as a functional moiety to boost and stabilise the antioxidant activities [49, 50]. Its integration as a base compound in the chemical synthesis of anticancer compounds is known to enhance bioefficacy against different cell lines [51, 52]. β-Sitosterol is a phytosterol for which the chemistry and pharmacology are fairly established. From various botanical sources, it is established to have analgesic, antimicrobial, anticancer, antidiabetic, anti-inflammatory, antioxidant, hypolipidemic, hepatoprotective and wound healing activities [53, 54]. It is considered as a prospective medication in several cancers including those of the breast, colon, leukaemia, lung, ovarian, prostate and stomach [55]. Its anticancer activity in particular has been vindicated from its molecular interactions with multiple cell signalling pathways involving

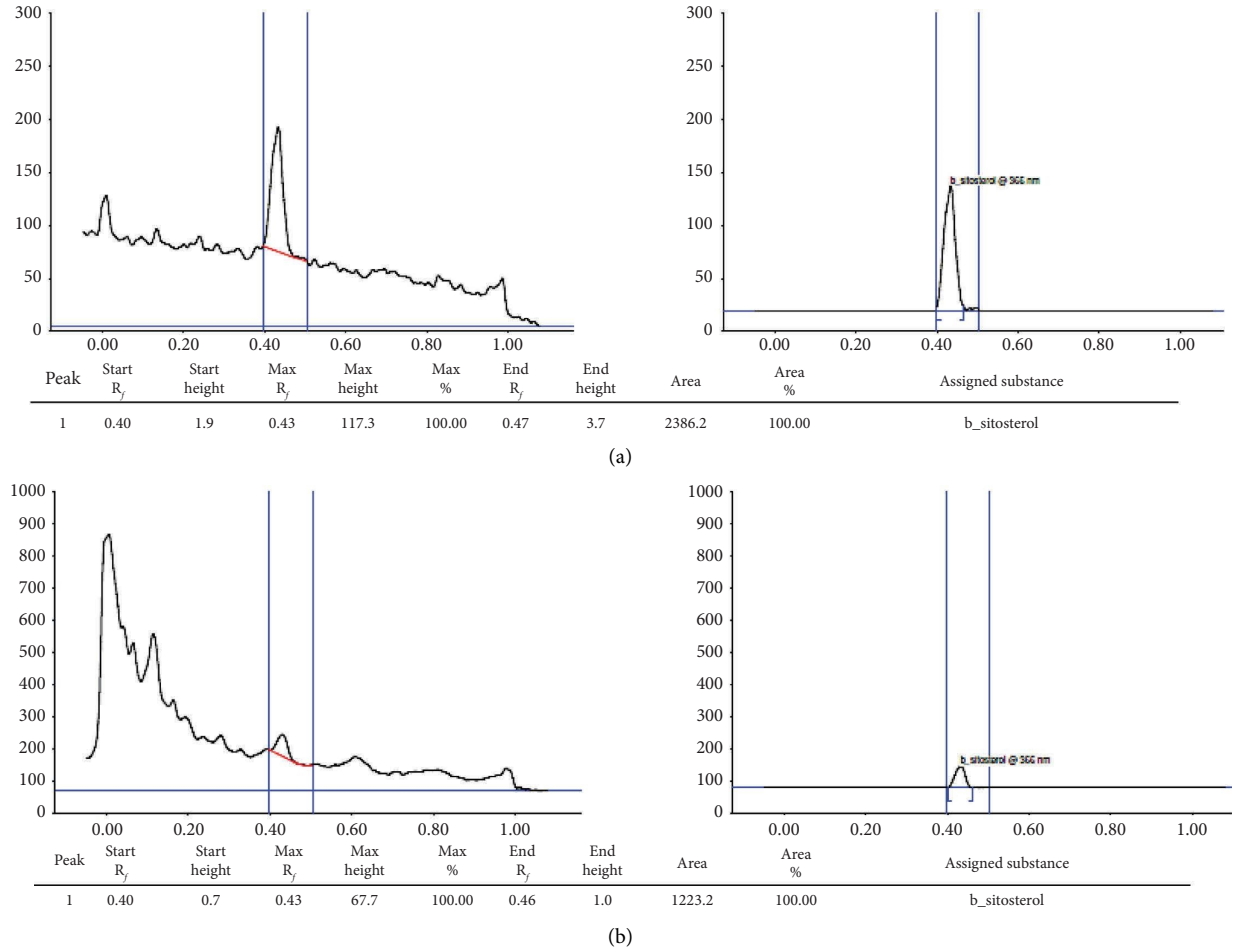

Figure 14: HPTLC chromatogram profiles. (a) Standard β-sitosterol detected at 366 nm and its respective R_f value. (b) β-Sitosterol in *I. khasiana* methanol–diethyl ether extract (IKM-D) detected at 254 nm and an R_f value of 0.43.

Table 11: Molecular data set-up for ligand-binding modelling in AutoDock Vina, showing the grid size, and centre position of compounds detected in *I. khasiana*.

Ligand	Size x	Size y	Size z	Centre x	Centre y	Centre z
2,6-Di-tert-butylphenol	70	62	60	136.118	104.379	17.042
β-Sitosterol	70	62	60	136.118	104.379	17.042

Table 12: Molecular docking scores of compounds detected in *I. khasiana* against common anticancer and anthelmintic target protein.

Ligand	Target	PDB code	Binding energy (kcal/mol)	Amino acid residue	Amino acid position
2,6-Di-tert-butylphenol	β-Tubulin	1SA0	−5.7	Glycine	146
β-Sitosterol	β-Tubulin	1SA0	−6.7	Alanine	100
				Alanine	180
				Valine	181
				Valine	182
				Phenylalanine	404
				Tryptophan	407

apoptosis, angiogenesis cell cycle, DNA repair and metastasis [56, 57].

Anthelmintic effects are most conveniently substantiated by electron microscopy and drug molecules primarily act on the body surface to induce tegumental disruptions [27, 28]. Furthermore, each anthelmintic drug exhibits characteristic and signature damaging effects on different body parts of helminths [58]. It is interesting to note that the most widely

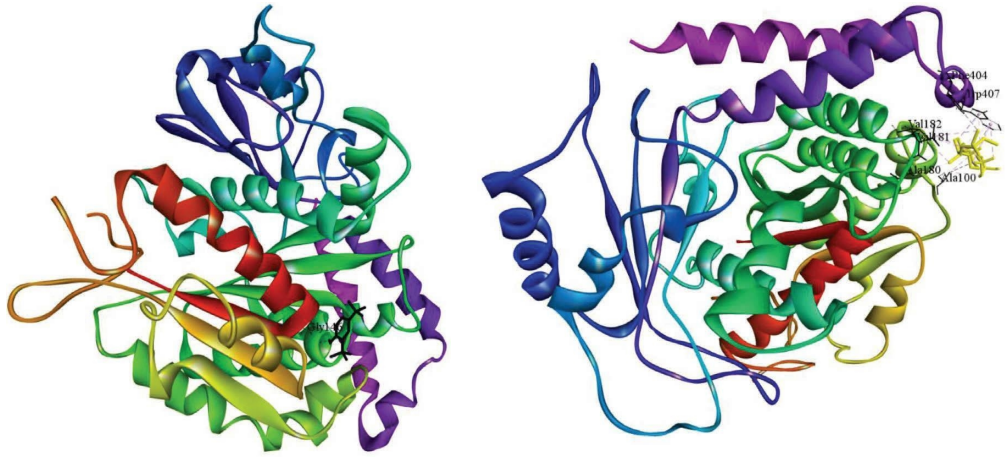

(a) (b)

Figure 15: 3D structural depiction of β-tubulin (PDB code 1SA0) shows the molecular interaction sites with major bioactive compounds detected in *I. khasiana* methanol–diethyl ether extract (IKM-D). (a) 2,6-Di-tert-butylphenol in black colour. (b) β-Sitosterol in yellow colour.

used anticancer drugs such as vinca alkaloids and paclitaxel share the same mechanisms of action as anthelmintic drugs such as albendazole. They are all inhibitors of tubulin assembly, the cellular process critical for normal microtubules during cell proliferation [4, 6, 59]. Molecular interactions showed that 2,6-di-tert-butylphenol and β-sitosterol do have high binding affinity for β-tubulin. The binding energy of each compound is not exceptionally high, but a strong deviation on the negative values is an indication of good binding interactions [60]. Therefore, the two compounds can specifically act as microtubule inhibitors by binding to free β-tubulins. Although it is by no means conclusive from the present findings that anticancer and anthelmintic activities of *I. khasiana* may have pharmacological activity consonant to the pharmaceutical drugs, it is enticing to infer that the plant's metabolites may act similarly to the drugs in causing the biological effects, and that 2,6-di-tert-butylphenol and β-sitosterol could potentially be the molecules behind the plant's anticancer and anthelmintic properties.

5. Conclusions

The methanol extract of *I. khasiana* leaves (IKM) and its fractions, including butanol (IKM-B), diethyl ether (IKM-D) and hexane (IKM-H), were found to exhibit in vitro anticancer activity against malignant type II human alveolar adenocarcinoma (A549) and human colon carcinoma (HCT116) cell lines. IKM-D showed the most pronounced cytotoxicity against both cell lines and was used for other biological and chemical analyses. The plant extract effectively exerted apoptosis as indicated by red fluorescence in the dead cells and high apoptotic index. Significant inhibition of cell proliferation and colony formation was also observed in IKM-D-treated cells. The plant extract further showed anthelmintic activity and caused typical drug effects on the tegument of cestode, as revealed by scanning electron microscopy. GC-MS data showed that the principal chemical compound in the plant extract was 2,6-di-tert-butylphenol. This phenolic compound may be the bioactive principle responsible for the anticancer and anthelmintic properties. β-Sitosterol was also identified using HPTLC fingerprinting. Both the detected compound can structurally interact with β-tubulin, which could be the molecular target for both anthelmintic and anticancer activities. The study hereof advocates the conservation and propagation of this endangered plant for any further pharmacological investigations.

Data Availability Statement

All the data used to support the findings of this study are included within the article.

Disclosure

The sponsor had no role in designing the research, data collection and analysis except in documenting the report.

Conflicts of Interest

The authors declare no conflicts of interest.

Author Contributions

Charles Lalnunfela performed the experiments, chemical analysis, analysed the data and prepared the first draft. Charles Lalnunfela assisted in the anticancer tests. P.B. Lalthanpuii performed anthelmintic tests, scanning electron microscopy and molecular docking. H.T. Lalremsanga and T.C. Lalhriatpuii conceived the project, supervised and procured research materials. T.C. Lalhriatpuii, Zothansiama, Kholhring Lalchhandama and N. Senthil Kumar designed the concepts and provided laboratory facilities. N. Senthil Kumar and Kholhring Lalchhandama acquired fundings for

the facilities. Kholhring Lalchhandama interpreted the data, structured the article and finalised the manuscript. All agreed to the article.

Funding

The study was supported by the DBT-BUILDER [BT/INF/22/SP41398/2021] scheme of the Department of Biotechnology, Government of India, established the DBT-BUILDER National Laboratory at Pachhunga University College and Advanced State Level Biotech Hub at Mizoram University.

Acknowledgments

The Department of Biotechnology, Government of India, established the DBT-BUILDER National Laboratory at Pachhunga University College and Advanced State Level Biotech Hub at Mizoram University.

References

[1] L. E. Navas and A. Carnero, "NAD^+ Metabolism, Stemness, the Immune Response, and Cancer," *Signal Transduction and Targeted Therapy* 6, no. 1 (2021): 2.

[2] D. Ajmeera and R. Ajumeera, "Drug Repurposing: A Novel Strategy to Target Cancer Stem Cells and Therapeutic Resistance," *Genes & Diseases* 11, no. 1 (2024): 148–175.

[3] S. Dallavalle, V. Dobričić, L. Lazzarato, et al., "Improvement of Conventional Anti-Cancer Drugs as New Tools Against Multidrug Resistant Tumors," *Drug Resistance Updates* 50 (2020): 100682.

[4] S. Chandra, M. Gahlot, A. N. Choudhary, et al., "Scientific Evidences of Anticancer Potential of Medicinal Plants," *Food Chemistry Advances* 2023 (2023): 100239.

[5] M. A. Ashraf, "Phytochemicals as Potential Anticancer Drugs: Time to Ponder Nature's Bounty," *BioMed Research International* 2020 (2020): 8602879.

[6] C. Zhang, M. Zhao, G. Wang, and Y. Li, "Recent Progress on Microtubule Degradation Agents," *Journal of Medicinal Chemistry* 66, no. 19 (2023): 13354–13368.

[7] F. A. Sofi and N. Tabassum, "Natural Product Inspired Leads in the Discovery of Anticancer Agents: An Update," *Journal of Biomolecular Structure and Dynamics* 41, no. 17 (2023): 8605–8628.

[8] P. Maleki Dana, F. Sadoughi, Z. Asemi, and B. Yousefi, "The Role of Polyphenols in Overcoming Cancer Drug Resistance: A Comprehensive Review," *Cellular & molecular Biology Letters* 27 (2022): 1–26.

[9] P. Garcia-Oliveira, P. Otero, A. G. Pereira, et al., "Status and Challenges of Plant-Anticancer Compounds in Cancer Treatment," *Pharmaceuticals* 14, no. 2 (2021): 157.

[10] X. Yao, F. Zhang, and R. T. Corlett, "Utilization of the Hollies (*Ilex* L. spp.): A Review," *Forests* 13, no. 1 (2022): 94.

[11] D. Hao, X. Gu, P. Xiao, Z. Liang, L. Xu, and Y. Peng, "Research Progress in the Phytochemistry and Biology of *Ilex* Pharmaceutical Resources," *Acta Pharmaceutica Sinica B* 3, no. 1 (2013): 8–19.

[12] S. Jiang, H. Cui, P. Wu, Z. Liu, and Z. Zhao, "Botany, Traditional Uses, Phytochemistry, Pharmacology and Toxicology of *Ilex pubescens* Hook et Arn," *Journal of Ethnopharmacology* 245 (2019): 112147.

[13] Q. Zhang, F. Feng, W. Y. Liu, and Q. L. Gu, "Two Triterpenoid Saponins With Anti-Tumor Activities on HepG2 and Other Compounds From *Ilex Pubescens*," *Chinese Journal of Natural Medicines* 8, no. 4 (2010): 253–256.

[14] J. R. Wang, H. Zhou, Z. H. Jiang, Y. F. Wong, and L. Liu, "In Vivo Anti-Inflammatory and Analgesic Activities of a Purified Saponin Fraction Derived From the Root of *Ilex Pubescens*," *Biological and Pharmaceutical Bulletin* 31, no. 4 (2008): 643–650.

[15] Q. Tan, M. Qiu, D. Cao, et al., "Triterpenoids with Antiplatelet Aggregation Activity from the Roots of *Ilex Pubescens*," *Planta Medica* 83, no. 9 (2017): 797–804.

[16] X. Fang, Y. Li, Y. Zheng, Y. Wang, S. Feng, and M. Miao, "Ethanol Extracts From *Ilex Pubescens* Promotes Cerebral Ischemic Tolerance via Modulation of TLR4-MyD88/TRIF Signaling Pathway in Rats," *Journal of Ethnopharmacology* 256 (2020): 112680.

[17] N. Bracesco, A. G. Sanchez, V. Contreras, T. Menini, and A. Gugliucci, "Recent Advances on *Ilex Paraguariensis* Research: Minireview," *Journal of Ethnopharmacology* 136, no. 3 (2011): 378–384.

[18] E. G. de Mejia, Y. S. Song, M. V. Ramirez-Mares, and H. Kobayashi, "Effect of Yerba Mate (*Ilex Paraguariensis*) Tea on Topoisomerase Inhibition and Oral Carcinoma Cell Proliferation," *Journal of Agricultural and Food Chemistry* 53, no. 6 (2005): 1966–1973.

[19] A. J. Saleh, L. Othman, M. Elchoueiry, et al., "Anti-Proliferative Activity of Yerba Mate (*Ilex Paraguariensis*) Aqueous Extracts on Human Colorectal Cancer Cell Lines," *Functional Foods in Health Diseases* 11, no. 10 (2021): 499–511.

[20] D. Adhikari, S. K. Barik, and K. Upadhaya, "Habitat Distribution Modelling for Reintroduction of *Ilex Khasiana* Purk., a Critically Endangered Tree Species of Northeastern India," *Ecological Engineering* 40 (2012): 37–43.

[21] C. Lalnunfela, H. T. Lalremsanga, T. C. Lalhriatpuii, D. Lalnunzira, and K. Lalchhandama, "Unveiling the Unexplored and Critically Endangered *Ilex Khasiana* for its Antioxidant Properties," *Journal of Natural Remedies* 19, no. 4 (2019): 214–220.

[22] C. Lalnunfela, P. B. Lalthanpuii, T. C. Lalhriatpuii, and K. Lalchhandama, "An Endangered Medicinal Plant, *Ilex Khasiana* Exhibits Potent Antiparasitic Activity Against Intestinal Tapeworm," *Pharmacognosy Journal* 12, no. 4 (2020): 725–730.

[23] C. Lalnunfela, H. T. Lalremsanga, T. C. Lalhriatpuii, P. B. Lalthanpuii, C. Lalmuanthanga, and K. Lalchhandama, "In Vivo Evaluation of *Ilex Khasiana* for its Analgesic and Anti-Inflammatory Activity on Swiss Albino Mice Model," *Indian Journal of Science and Technology* 16 (2023): 39–47.

[24] T. Mosmann, "Rapid Colorimetric Assay for Cellular Growth and Survival: Application to Proliferation and Cytotoxicity Assays," *Journal of Immunological Methods* 65, no. 1–2 (1983): 55–63.

[25] C. Gill, C. L. Fischer, and L. A. Cone, "Lymphocyte-Mediated Cytotoxicity Microassay by Cytofluorography," *Journal of Immunological Methods* 25, no. 1 (1979): 21–30.

[26] A. W. Hamburger and S. E. Salmon, "Primary Bioassay of Human Tumor Stem Cells," *Science* 197, no. 4302 (1977): 461–463.

[27] P. B. Lalthanpuii, Z. Zokimi, and K. Lalchhandama, "The Toothache Plant (*Acmella Oleracea*) Exhibits Anthelmintic Activity on Both Parasitic Tapeworms and Roundworms," *Pharmacognosy Magazine* 16, no. 1 (2020): 193–198.

[28] K. Lalchhandama, "In Vitro Effects of Albendazole on Raillietina echinobothrida, the Cestode of Chicken, Gallus domesticus," *Journal of Young Pharmacists* 2, no. 4 (2010): 374–378.

[29] E. Tyihák, E. Mincsovics, and H. Kalász, "New Planar Liquid Chromatographic Technique: Overpressured Thin-Layer Chromatography," *Journal of Chromatography A* 174, no. 1 (1979): 75–81.

[30] R. B. Ravelli, B. Gigant, P. A. Curmi, et al., "Insight into Tubulin Regulation From a Complex With Colchicine and a Stathmin-Like Domain," *Nature* 428, no. 6979 (2004): 198–202.

[31] S. Tang, R. Chen, M. Lin, et al., "Accelerating AutoDock Vina With GPUs," *Molecules* 27, no. 9 (2022): 3041.

[32] Y. Katakura, "Molecular Basis for the Cellular Senescence Program and its Application to Anticancer Therapy," *Bioscience, Biotechnology, and Biochemistry* 70, no. 5 (2006): 1076–1081.

[33] D. Pal, I. Song, S. D. Warkad, et al., "Indazole-Based Microtubule-Targeting Agents as Potential Candidates for Anticancer Drugs Discovery," *Bioorganic Chemistry* 122 (2022): 105735.

[34] T. Noureddine, Z. El Husseini, A. Nehme, and R. A. Massih, "Antibacterial Activity of *Ilex Paraguariensis* (Yerba Mate) against Gram-Positive and Gram-Negative Bacteria," *The Journal of Infection in Developing Countries* 12, no. 9 (2018): 712–719.

[35] D. H. Bastos, L. A. Saldanha, R. R. Catharino, et al., "Phenolic Antioxidants Identified by ESI-MS From Yerba Mate (*Ilex Paraguariensis*) and Green Tea (*Camelia sinensis*) Extracts," *Molecules* 12, no. 3 (2007): 423–432.

[36] M. Alam, S. Ahmed, A. M. Elasbali, et al., "Therapeutic Implications of Caffeic Acid in Cancer and Neurological Diseases," *Frontiers in Oncology* 12 (2022): 860508.

[37] E. G. de Mejía, Y. S. Song, C. I. Heck, and M. Ramírez-Mares, "Yerba Mate Tea (*Ilex Paraguariensis*): Phenolics, Antioxidant Capacity and *In Vitro* Inhibition of Colon Cancer Cell Proliferation," *Journal of Functional Foods* 2, no. 1 (2010): 23–34.

[38] M. Amigo-Benavent, S. Wang, R. Mateos, B. Sarriá, and L. Bravo, "Antiproliferative and Cytotoxic Effects of Green Coffee and Yerba Mate Extracts, Their Main Hydroxycinnamic Acids, Methylxanthine and Metabolites in Different Human Cell Lines," *Food and Chemical Toxicology* 106 (2017): 125–138.

[39] G. D. Noratto, Y. Kim, S. T. Talcott, and S. U. Mertens-Talcott, "Flavonol-Rich Fractions of Yaupon Holly Leaves (*Ilex Vomitoria*, Aquifoliaceae) Induce microRNA-146a and Have Anti-inflammatory and Chemopreventive Effects in Intestinal Myofribroblast CCD-18Co Cells," *Fitoterapia* 82, no. 4 (2011): 557–569.

[40] X. Zhao, Q. Wang, Y. Qian, and J. L. Song, "Ilex Kudingcha CJ Tseng (Kudingcha) Has In Vitro Anticancer Activities in MCF-7 Human Breast Adenocarcinoma Cells and Exerts Anti-metastatic Effects In Vivo," *Oncology Letters* 5, no. 5 (2013): 1744–1748.

[41] K. Zhu, G. Li, P. Sun, R. Wang, Y. Qian, and X. Zhao, "In Vitro And In Vivo Anti-Cancer Activities of Kuding Tea (Ilex Kudingcha CJ Tseng) Against Oral Cancer," *Experimental and Therapeutic Medicine* 7, no. 3 (2014): 709–715.

[42] Y. Zhang, H. Yang, W. Sun, et al., "Ethanol Extract of *Ilex Hainanensis* Merr. Exhibits Anti-Melanoma Activity by Induction of G 1/S Cell-Cycle Arrest and Apoptosis," *Chinese Journal of Integrative Medicine* 24 (2018): 47–55.

[43] T. Hu, X. W. He, and J. G. Jiang, "Functional Analyses on Antioxidant, Anti-Inflammatory, and Antiproliferative Effects of Extracts and Compounds from *Ilex Latifolia* Thunb., a Chinese Bitter Tea," *Journal of Agricultural and Food Chemistry* 62, no. 34 (2014): 8608–8615.

[44] W. J. Liu, Y. Y. Peng, H. Chen, X. F. Liu, J. Y. Liang, and J. B. Sun, "Triterpenoid Saponins With Potential Cytotoxic Activities From the Root Bark of *Ilex Rotunda* Thunb," *Chemistry and Biodiversity* 14, no. 2 (2017): e1600209.

[45] E. Agathokleous, C. Saitanis, and A. Markouizou, "Hormesis Shifts the No-Observed-Adverse-Effect Level (NOAEL)," *Dose-Response* 19, no. 1 (2021): 15593258211001667.

[46] A. Murakami, "Novel Mechanisms Underlying Bioactivities of Polyphenols via Hormesis," *Current Opinion in Toxicology* 30 (2022): 100337.

[47] D. Rizwan and F. A. Masoodi, "Brassica-derived Isothiocyanates as Anticancer Therapeutic Agents and Their Nanodelivery," *Phytotherapy Research* 38, no. 1 (2024): 331–348.

[48] F. Zhao, P. Wang, R. D. Lucardi, Z. Su, and S. Li, "Natural Sources and Bioactivities of 2, 4-Di-Tert-Butylphenol and its Analogs," *Toxins* 12, no. 1 (2020): 35.

[49] S. S. Shatokhin, V. A. Tuskaev, S. C. Gagieva, et al., "Synthesis, Cytotoxic and Antioxidant Activities of New *N*-Substituted 3-(benzimidazol-2-Yl)-Chromones Containing 2, 6-Di-Tert-Butylphenol Fragment," *Journal of Molecular Structure* 1249 (2022): 131683.

[50] T. A. Antonenko, D. B. Shpakovsky, M. A. Vorobyov, et al., "Antioxidative vs Cytotoxic Activities of Organotin Complexes Bearing 2, 6-di-tert-butylphenol Moieties," *Applied Organometallic Chemistry* 32, no. 7 (2018): e4381.

[51] E. R. Milaeva, D. B. Shpakovsky, Y. A. Gracheva, et al., "Novel Selective Anticancer Agents Based on Sn and Au Complexes. Mini-Review," *Pure and Applied Chemistry* 92, no. 8 (2020): 1201–1216.

[52] S. Braun, S. Jelača, M. Laube, et al., "Synthesis and In Vitro Biological Evaluation of P-Carborane-Based Di-tert-butylphenol Analogs," *Molecules* 28, no. 11 (2023): 4547.

[53] S. Babu and S. Jayaraman, "An Update on β-Sitosterol: A Potential Herbal Nutraceutical for Diabetic Management," *Biomedicine & Pharmacotherapy* 131 (2020): 110702.

[54] P. Yadav, C. Chauhan, S. Singh, S. Banerjee, and K. Murti, "β-Sitosterol in Various Pathological Conditions: An Update," *Current Bioactive Compounds* 18, no. 6 (2022): 19–27.

[55] S. Nandi, A. Nag, S. Khatua, et al., "Anticancer Activity and Other Biomedical Properties of β-Sitosterol: Bridging Phytochemistry and Current Pharmacological Evidence for Future Translational Approaches," *Phytotherapy Research* 38, no. 2 (2024): 592–619.

[56] Z. Khan, N. Nath, A. Rauf, et al., "Multifunctional Roles and Pharmacological Potential of β-sitosterol: Emerging Evidence Toward Clinical Applications," *Chemico-Biological Interactions* 365 (2022): 110117.

[57] X. Bao, Y. Zhang, H. Zhang, and L. Xia, "Molecular Mechanism of β-Sitosterol and its Derivatives in Tumor Progression," *Frontiers in Oncology* 12 (2022): 926975.
[58] P. B. Lalthanpuii and K. Lalchhandama, "Scanning Electron Microscopic Study of the Anthelmintic Effects of Some Anthelmintic Drugs on Poultry Nematode, *Ascaridia galli*," *Advances in Animal and Veterinary Sciences* 8, no. 8 (2020): 788–793.
[59] J. Y. Chai, B. K. Jung, and S. J. Hong, "Albendazole and Mebendazole as Anti-Parasitic and Anti-Cancer Agents: an Update," *Korean Journal of Parasitology* 59, no. 3 (2021): 189.
[60] L. Zheng, J. Meng, K. Jiang, et al., "Improving Protein-Ligand Docking and Screening Accuracies by Incorporating a Scoring Function Correction Term," *Briefings in Bioinformatics* 23, no. 3 (2022): 51.